Published in final edited form as:
Exp Neurol. 2011 August ; 230(2): 258–272. doi:10.1016/j.expneurol.2011.05.004.

Some lumbar sympathetic neurons develop a glutamatergic phenotype after peripheral axotomy with a note on $VGLUT_2$-positive perineuronal baskets

Pablo R. Brumovsky[1,2,*], **Kim B. Seroogy**[3], **Kerstin H. Lundgren**[3], **Masahiko Watanabe**[4], **Tomas Hökfelt**[5], and **G. F. Gebhart**[1]

[1]Pittsburgh Center for Pain Research, Department of Anesthesiology, University of Pittsburgh, Pittsburgh, PA 15213

[2]Faculty of Biomedical Sciences, Austral University, Buenos Aires, B1629AHJ, Argentina

[3]Department of Neurology, University of Cincinnati, Cincinnati, OH 45267

[4]Department of Anatomy, Hokkaido University School of Medicine, Japan

[5]Department of Neuroscience, Karolinska Institutet, Stockholm, SE 17177, Sweden

Abstract

Glutamate is the main excitatory neurotransmitter in the nervous system, including in primary afferent neurons. However, to date a glutamatergic phenotype of autonomic neurons has not been described. Therefore, we explored the expression of vesicular glutamate transporters (VGLUTs) type 1, 2 and 3 in lumbar sympathetic chain (LSC) and major pelvic ganglion (MPG) of naïve BALB/C mice, as well as after pelvic nerve axotomy (PNA), using immunohistochemistry and in situ hybridization. Colocalization with activating transcription factor-3 (ATF-3), tyrosine hydroxylase (TH), vesicular acetylcholine transporter (VAChT) and calcitonin generelated peptide was also examined. Sham-PNA, sciatic nerve axotomy (SNA) or naïve mice were included. In naïve mice, $VGLUT_2$-like immunoreactivity (LI) was only detected in fibers and varicosities in LSC and MPG; no ATF-3-immunoreactive (IR) neurons were visible. In contrast, PNA induced upregulation of $VGLUT_2$ protein and transcript, as well as of ATF-3-LI in subpopulations of LSC neurons. Interestingly, $VGLUT_2$-IR LSC neurons coexpressed ATF-3, and often lacked the noradrenergic marker TH. SNA only increased $VGLUT_2$ protein and transcript in scattered LSC neurons. Neither PNA nor SNA upregulated $VGLUT_2$ in MPG neurons. We also found perineuronal baskets immunoreactive either for $VGLUT_2$ or the acetylcholinergic marker VAChT in non-PNA MPGs, usually around TH-IR neurons. $VGLUT_1$-LI was restricted to some varicosities in MPGs, was absent in LSCs, and remained largely unaffected by PNA or SNA. This was confirmed by the lack of expression of $VGLUT_1$ or $VGLUT_3$ mRNAs in LSCs, even after PNA or SNA. Taken together, axotomy of visceral and non-visceral nerves results in a glutamatergic phenotype of some LSC neurons. In addition, we show previously non-described MPG perineuronal glutamatergic baskets.

[*]**Corresponding author**[1]: P. R. Brumovsky, Center for Pain Research, University of Pittsburgh Medical Center, University of Pittsburgh, 200 Lothrop Street, W1402BST, Pittsburgh 15213, USA, brumovskypr@upmc.edu; pbrumovs@cas.austral.edu.ar.
[1]Current address: Faculty of Biomedical Sciences, Av. Juan D. Perón 1500, B1629AHJ, Austral University, Buenos Aires, Argentina; Phone: 54 2322 48 2699

Keywords

autonomic neurons; axotomy; glutamate; neuropeptides; pain; pelvic nerve; sensory neurons; vesicular glutamate transporter

Introduction

Vesicular glutamate transporters (VGLUTs) incorporate the excitatory neurotransmitter glutamate into synaptic vesicles, and three subtypes have been identified to date, $VGLUT_1$, $VGLUT_2$ and $VGLUT_3$ (Kaneko and Fujiyama 2002; Fremeau, Jr. et al., 2004; Liguz-Lecznar and Skangiel-Kramska 2007). VGLUTs are tightly related to the glutamatergic neuronal phenotype and have become standard markers for the study of neurons using glutamate as neurotransmitter (see Brumovsky et al., 2007). Their expression has been analyzed in detail in rodent dorsal root ganglion (DRG) sensory neurons innervating non-visceral structures like skin (Oliveira et al., 2003; Hwang et al., 2004; Landry et al., 2004; Morris et al., 2005; Brumovsky et al., 2007; Seal et al., 2009), where $VGLUT_2$ appears to be the most abundantly expressed transporter (Morris et al., 2005; Brumovsky et al., 2007). We also have detected expression of $VGLUT_2$, and to a lesser extent $VGLUT_1$, in DRG neurons retrogradely traced from the mouse colorectum (unpublished data), in agreement with the presence of $VGLUT_1$ and $VGLUT_2$ protein in nerve fibers innervating guinea pig (Olsson et al., 2004) and mouse (Spencer et al., 2008) rectum.

Visceral organs like the colorectum are innervated in rodents by: 1) peripheral projections of thoracolumbar and lumbosacral DRG neurons (see Robinson and Gebhart 2008); 2) postganglionic projections of sympathetic neurons contained in the lumbar sympathetic chain (LSC); 3) sympathetic and parasympathetic neurons present in the ‘mixed’ major pelvic ganglion (MPG) (Furness 2006; Keast 2006), and 4) enteric neurons, residing within the gut walls and creating an ‘intrinsic’ sensory and motor neuronal network (Furness et al., 2004). Peripheral afferent sensory, postganglionic sympathetic and preganglionic parasympathetic efferent axons innervating these organs travel together in the pelvic (PN) and lumbar splanchnic (LSN) nerves. The effects of injuries to these nerves have not been thoroughly explored.

The pathophysiology of non-visceral pain induced by peripheral nerve lesion has been intensely studied over the last few decades. Several models are utilized in rodents and include complete axotomy (Wall et al., 1979), different types of compression of the sciatic nerve (Bennett and Xie 1988; Brumovsky et al., 2004) as well as section of nerve branches (see Jaggi et al., 2011). These procedures are well known to induce a complex array of up- and downregulation of a variety of molecules in their respective cell somata in DRG (e.g. sodium and potassium channels, neuropeptides, neurotrophic factors and their receptors, and inflammation-associated receptors (Xiao et al., 2002; Costigan et al., 2002; Navarro et al., 2007)). Recently, changes in the expression of VGLUTs in DRG neurons of rat and mouse have also been described (Hughes et al., 2004; Brumovsky et al., 2007).

Sympathetic neurons are classically identified by their expression of the noradrenergic marker tyrosine hydroxylase (TH) (Apostolova and Dechant 2009), but are also capable of synthesizing a diversity of neurotransmitters, including acetylcholine and neuropeptides (Elfvin et al., 1993; Zigmond and Sun 1997; Landry et al., 2000; Navarro et al., 2007). Interestingly, the possibility of a glutamatergic phenotype for autonomic neurons has not previously been reported. Sympathetic neurons are also affected by axotomy of their postganglionic projections (see (Zigmond and Sun 1997; Landry et al., 2000; Navarro et al., 2007)). Thus, downregulation of the neuropeptide tyrosine (NPY) or TH (Cheah and Geffen

1973; Sun and Zigmond 1996; Zigmond and Sun 1997; Landry et al., 2000; Navarro et al., 2007), and upregulation of galanin (Lindh et al., 1993; Zigmond and Sun 1997; Landry et al., 2000; Navarro et al., 2007), vasoactive intestinal peptide (VIP) and substance P (SP) (Rao et al., 1993; Zigmond and Sun 1997; Landry et al., 2000; Navarro et al., 2007) have been shown in superior cervical ganglion neurons after axotomy of their projections in rodents. Similar effects on some of the neurotransmitters mentioned above have also been shown in cat LSC (Lindh et al., 1993). Many of these neurochemical changes could relate to neuropathic pain mechanisms after nerve injury by sympathetic-sensory coupling (Shinder et al., 1999; Habler et al., 2000; Jänig 2003; Gibbs et al., 2008). Thus, identification of key sensory and autonomic molecules participating in the generation, maintenance or attenuation of pain remains essential for the development of novel analgesic/regenerative drugs.

To date a glutamatergic phenotype of autonomic neurons has not been studied. Here we use VGLUT1-3 as selective markers of a glutamatergic phenotype for analysis of mouse LSC and MPG, before and after pelvic nerve axotomy (PNA). The widely utilized sciatic nerve axotomy (SNA) model was also included. Colocalization analysis using antibodies raised against TH, the vesicular acetylcholine transporter (VAChT) and calcitonin gene-related peptide (CGRP) were also performed. Finally, we evaluated the expression of transcripts for $VGLUT_1$, $VGLUT_2$ and $VGLUT_3$ in the LSC and MPG, to compare with the immunohistochemical data, and to compensate for the lack of a reliable $VGLUT_3$ antibody.

Experimental Procedures

Animals

Male BALB/c mice (Taconic, Germantown, NJ or Jackson Laboratories, Bar Harbor, Maine, USA; 7–8 weeks old) were used. Experiments adhered to the United States Public Health Service policies regarding the care and use of animals in research, followed the Uniform Requirements for manuscripts submitted to Biomedical journals and were approved by the Institutional Animal Care Use Committee (University of Pittsburgh).

Pelvic or sciatic nerve axotomy

(Fig. 1). Axotomy of the pelvic nerve (PN) in mouse is complicated by the proximity of the bifurcation of the aorta into the iliac arteries and thus difficult to execute without damaging other tissues. Thus, an alternative approach was taken to transect major contributing nerves, which we refer to for convenience throughout this report as PNA (PN axotomy). In twelve isoflurane-anesthetized mice (Hospira Inc, Lake Forest, IL USA) injected with buprenorphine (0.1 mg/kg; Bedford Labs, Bedford, OH, USA) for postoperative analgesia, the ventral branches of the left 6^{th} lumbar and 1^{st} sacral spinal nerves, both major contributors to the PN, were exposed by aseptic laparotomy and dissection (S2 also contributes some fibers, but their percentage is very small and could be considered less relevant than L6 or S1). In eight mice, we tightly ligated and distally axotomized these two spinal nerves contributing to the PN (i.e., PNA); in the remaining four mice the same spinal nerves were exposed as described, but left intact (sham group). After suturing of the abdominal wall and topical application of 1% dibucaine ointment (1%; Perrigo, Allegan, MI, USA), mice recovered in a warm environment.

Additional mice were subjected to tight ligation and axotomy of the sciatic nerve (SNA; n=8) or sham surgery (n=4) as previously described (see Brumovsky et al., 2007) for comparison with the effects of PNA on LSC and MPG neurons.

Immunohistochemistry

Seven (PNA) or ten (SNA) days after lesion, mice were deeply anaesthetized using sodium pentobarbital (60 mg/kg, i.p.; Ovation Pharmaceuticals, Deerfield, IL) and perfused via the ascending aorta with 20 ml of Tyrode's buffer (37°C), followed by 20 ml of a mixture of 4% paraformaldehyde and 0.2% picric acid dissolved in 0.16 M phosphate buffer (pH 6.9) (37°C) and 50 ml of the same mixture at 4°C, the latter for approximately 5–7 min (Zamboni and De Martino 1967). Four naïve mice were also included. The ipsilateral and contralateral LSCs and MPGs were dissected out and post fixed for 90 min at 4°C in the same fixative and finally immersed in 10–20% sucrose in phosphate-buffered saline (PBS) (pH 7.4) containing 0.01% sodium azide and 0.02% bacitracin (both from Sigma, St. Louis, MO) (4°C) for 48 h. After embedding in Tissue-Tek O.C.T. compound (Sakura, Torrence, CA) and deep freezing, all tissues were sectioned in a cryostat (Leica, Heidelberg, Germany) at 12 μm (LSC) or 20 μm thicknesses (MPG).

Tissue sections were incubated in a series of primary and secondary antibodies (Table 1), according to the tyramide signal amplification technique (Adams 1992) for single-staining immunohistochemistry, and following a previously described protocol (see (Brumovsky et al., 2007)). The $VGLUT_1$ and $VGLUT_2$ antibodies were raised against the C-terminal sequence of mouse $VGLUT_1$ [531–560 amino acid residues, GeneBank accession number U07609 (Kawamura et al., 2006; Miura et al., 2006)] or mouse $VGLUT_2$ [549–582 amino acid residues, GeneBank accession number BC038375 (Miyazaki et al., 2003)] and were expressed as glutathione-S transferase fusion proteins for immunization. Antibody specificity was tested by immunoblot of mouse brain extracts, with detection of a single band at 60kDa for both $VGLUT_1$ and $VGLUT_2$ (Miyazaki et al., 2003; Kawamura et al., 2006; Miura et al., 2006), and also by immunostaining patterns in the adult mouse brain, which were identical to previous reports by immunohistochemistry and *in situ* hybridization.

Some sections underwent additional primary and secondary antibody incubation steps (Table 1) for double- or triple-staining, following the protocol of indirect immunofluorescence by Coons and collaborators (see Coons 1958) or additional TSA protocols (see Brumovsky et al., 2007). LSC sections were also incubated with DAPI, for the identification of the nuclear profiles of all cells present per section (Kubista et al., 1987).

Specificity of the $VGLUT_2$ antibody has been previously tested (Kawamura et al., 2006; Brumovsky et al., 2007). The rabbit $VGLUT_1$ antiserum was studied after preadsorption with the C-terminal 531–560 amino acid peptide (10^{-5} and 10^{-6}M), this combination giving no visible fluorescent signal (data not shown). ATF-3, TH, VAChT and CGRP antibodies are commercially available and repeatedly validated. Additional control experiments included the comparison of single- and double-stained sections; and the omission of the primary antibody in a few sections to test for non-specific staining by the secondary antibodies.

Riboprobe *in situ* hybridization

Male, 7 week old, BALB/c mice (PNA=4; sham-PNA=2; SNA=4; sham-SNA=2; naïve=2) were used for *in situ* hybridization analysis. Mice were sedated using CO_2 before rapid decapitation. The LSC and the MPG were quickly removed, embedded in O.C.T. (Tissue-Tek, Sakura, Torrance, CA) and frozen over dry ice. Sections of LSCs and MPGs (12 μm and 20 μm, respectively) were cut in a cryostat, thaw-mounted onto Superfrost Plus (Fisher Scientific, Waltham, MA) glass slides, and stored at −20°C until hybridization. Adjacent sections through the different tissues were processed for *in situ* hybridization localization of $VGLUT_1$, $VGLUT_2$ and $VGLUT_3$ mRNAs, using ^{35}S-labeled cRNA probes as described previously (Seroogy and Herman 1997; Numan et al., 2005; Dickerson et al., 2009).

Sense and antisense probes complementary to the coding region of mouse VGLUTs were generously provided by Drs. Akiya Watakabe, National Institute for Basic Biology, Okazaki, Japan [$VGLUT_1$, and $VGLUT_2$ (Nakamura et al., 2007)] and Jeffery Erickson, Louisiana State University, Baton Rouge, LA [$VGLUT_3$ (Schäfer et al., 2002)]. The sense and antisense cRNA probes were prepared by *in vitro* transcription using appropriate linearized DNA constructs in the presence of the proper RNA polymerase (T3, T7, or SP6) and ^{35}S-UTP (PerkinElmer, Chelton, CT).

Hybridized sections were dipped in NTB2 nuclear track emulsion (Kodak, City, State; 1:1 in dH_2O), air-dried, and exposed in sealed slide boxes at 4°C for 3 and 7 days for brain and brainstem or LSC and MPG sections, respectively. The emulsion was developed in D19 (Kodak) and fixed with Rapidfix (Kodak). The slides were counterstained with cresyl violet (Sigma) and coverslipped with DPX mounting solution (Fluka, Saint Louis, MO).

As controls for specificity, some sections were pretreated with ribonuclease A (0.05 mg/mL) for 30 min at 45°C before hybridization with the ^{35}S-labeled cRNA probes. Some sections were also hybridized with sense-strand ^{35}S-labeled riboprobes against each VGLUT. Finally, several tissue sections were incubated in hybridization cocktail that lacked the radioactive probe as a chemography control. No specific labeling was observed under any of these control conditions.

Microscopy and image processing

Sections processed for immunofluorescence were cover-slipped using 2.5% DABCO in glycerol (Sigma) and examined using a Nikon Eclipse E600 fluorescence microscope (Nikon, Tokyo, Japan) provided with appropriate objectives, filters and a Retiga 2000 R Fast CCD camera (Q-Imaging, Surrey, BC, Canada), using IPLab software (Scanalytics Inc., Vancouver, BC, Canada). For colocalization analysis, a Fluoview FV 1000 confocal laser scanning biological microscope equipped with 10× (0.45 N.A.), 20× (0.75 N.A.) and 60× oil (1.40 N.A.) objectives was used (Olympus, Tokyo, Japan). The FITC labelling was excited using a 547-514 nm argon multi-line laser. For the detection of TRITC and TMR, the 543 nm HeNe laser was used.

Sections processed for riboprobe *in situ* hybridization were examined using a Nikon Eclipse E800 fluorescence microscope provided with appropriate objectives and filters for bright- and dark-field visualization, and a DN100 Nikon Digital Net Camera.

Resolution, brightness and contrast of the images were optimized using the Adobe Photoshop CS3 software (Adobe Systems Inc., San Jose, CA).

Quantification and statistical analysis

Every fifth LSC section was used to quantify the number of $VGLUT_1$, $VGLUT_2$ or $VGLUT_3$ mRNA positive neuron profiles (NPs), as well as the total number of cresyl violet-stained NPs, giving a typical nuclear staining. Only nucleated NPs were counted. In total, 5 sections per LSC were used for quantification. An average of 752 NPs per mouse was counted in this study.

Data are presented as mean ± SEM and were statistically analyzed using the Student t test.

Results

Pelvic nerve axotomy induces upregulation of $VGLUT_2$ protein and mRNA, but not $VGLUT_1$ or $VGLUT_3$, in LSC NPs

In LSCs from naïve (Fig. 2A), as well as in contralateral sham-PNA, PNA or SNA mice (data not shown), $VGLUT_1$-like immunoreactivity (LI) was virtually absent, as it also was after PNA (Fig. 2B). Some $VGLUT_2$-immunoreactive (IR) fibers and varicosities, but no neuronal cell bodies, were detected in LSCs from naïve mice (Fig. 2C) and in contralateral LSCs from mice subjected to sham-PNA (Fig. 3A), PNA or SNA (data not shown). In contrast, PNA induced upregulation of $VGLUT_2$-LI in a considerable number of LSC neurons (Fig. 3C). This was accompanied by a dramatic upregulation of ATF-3-LI in LSC neurons (Fig. 3D), as compared to its absence in contralateral LSCs from sham-PNA (Fig. 3B), naïve or contralateral LSCs from PNA and SNA mice (data not shown). Sham-PNA (Fig. 3E–H) induced at most a moderate, variable upregulation of $VGLUT_2$ in LSC NPs-LI (Fig. 3E, G) and $VGLUT_2$ transcript (Fig. 4C, D), with parallel increases in the number of ATF-3-IR NPs (Fig. 3F, H).

Quantification of the number of NPs upregulating VGLUTs in the LSC was done on riboprobe *in situ* hybridization-processed slides (Table 2). We found that $VGLUT_2$ mRNA was also absent in naïve LSC (Table 2; Fig. 4A, B), and only detected in occasional NPs in the ipsilateral side of sham-PNA mice (Table 2; Fig. 4C, D). In contrast, PNA induced a marked upregulation of $VGLUT_2$-mRNA-positive LSC NPs (Table 2; Fig. 4E, F), whereas SNA resulted in a more modest upregulation than after PNA (Table 2; Fig. 4G, H). Overall, the grain density of upregulated $VGLUT_2$ riboprobe labeling after PNA (Fig. 4E, F) or SNA (Fig. 4G, H) appeared to vary from medium to strong, and clearly differentiated from the surrounding background grain density. However, a few NPs showing a lesser grain density related to $VGLUT_2$ mRNA were also detected in the ipsilateral LSC of sham-PNA mice (Fig. 4C, D), as well as in some NPs after PNA (Fig. 4E, F) or SNA (Fig. 4G, H). Certifying the sensitivity and specificity of the $VGLUT_2$ riboprobe, its application to brainstem sections showed established and abundant labeling in regions such as the periaqueductal gray (Fig. 4J) (Lein et al., 2007; Ng et al., 2009).

As observed with immunohistochemistry, $VGLUT_1$- (Table 2; Fig. 5A) and $VGLUT_3$- (Table 2; Fig. 5B) mRNA-positive NPs are absent in naïve LSC. Likewise, sham-PNA (Fig. 5C, D), PNA (Fig. 5E, F) or SNA (Fig. 5G, H) failed to induce any change in the expression of either transcript. The riboprobes for $VGLUT_1$ or $VGLUT_3$ mRNAs did, however, efficiently label neurons in brain regions such as the hippocampus (Fig. 5I) and the dorsal raphe nucleus (Fig. 4K), respectively (cf. Lein et al., 2007; Ng et al., 2009).

Hybridization of brain sections with appropriate control sense riboprobes resulted in absence of the normal labeling patterns previously published and shown in the present study (compare Fig. 5I, J for $VGLUT_1$; Fig. 5K, L for $VGLUT_3$; and Fig. 4E, I and J, K for $VGLUT_2$).

$VGLUT_2$ protein is selectively upregulated in axotomized LSC neurons

Colocalization analysis showed that virtually all $VGLUT_2$-IR neurons in LSCs ipsilateral to PNA (Fig. 6A–C), SNA (Fig. 6D–I) or sham-PNA (Fig. 6J–L), as well as rare NPs found contralateral to a sham-PNA (Fig. 6M–O), also upregulated ATF-3, a marker of mechanically injured neurons (Tsujino et al., 2000).

Colocalization analysis with TH revealed that the great majority of the $VGLUT_2$-IR neurons in LSCs from PNA mice (Fig. 7A–I) appeared to lack the noradrenergic marker. However, a few neurons clearly coexpressing both $VGLUT_2$ and TH could be detected (Fig. 7D–I). TH-

positive neurons were either strongly or weakly immunoreactive (Fig. 7B, E, H), but the few somata co-expressing $VGLUT_2$-IR most often belonged to the second group (Fig. 7G–I). In LSCs ipsilateral to a sham-PNA (Fig. 7J–L) or SNA (data not shown), the few neurons upregulating $VGLUT_2$ also lacked TH-LI, with the exception of occasional neurons positive for both markers (Fig. 7J–L). In LSCs contralateral to sham-PNA (Fig. 7M–R), PNA or SNA mice (data not shown), thick $VGLUT_2$-IR, TH-negative nerve bundles could be seen in close association with the LSC, apparently projecting smaller bundles towards the ganglion (Fig. 7M–O). Occasionally, clusters of perineuronal baskets formed by $VGLUT_2$-IR varicosities surrounded TH-IR LSC neurons in the contralateral LSC of a sham-PNA mouse (Fig. 7P–R).

$VGLUT_2$-IR perineuronal baskets, present in the mouse MPG, lack CGRP, VAChT and TH

In MPGs from contralateral (Figs. 8AF) or ipsilateral (Figs. 9E–L) sham-PNA, or contralateral PNA (Figs. 9A–D, M–P), $VGLUT_2$-LI was often detected in nerve fibers (Figs. 8A–C; 9A–D), as was as in perineuronal baskets built up of varicose nerve endings (Figs. 8A–F; 9E–P). $VGLUT_1$-LI was confined to a few varicosities sparsely distributed throughout the ganglion, as observed in contralateral PNA (Fig. 10A) or ipsilateral sham-PNA (Fig. 10C).

Colocalization analysis showed that the $VGLUT_2$-IR baskets in the MPG virtually never colocalize with CGRP (Fig. 8A–F), although $VGLUT_2$- and CGRP-IRs intermingled in nerve bundles in this ganglion, possibly partly coexisting (Fig. 8D–F). $VGLUT_2$-IR perineuronal baskets were often detected around TH-IR MPG neurons (Fig. 9A–P), although some were occasionally found around neurons negative for the noradrenergic marker (data not shown). Colocalization analysis with VAChT (Fig. 9B, F, J) and TH (Figs. 9C, G, K) showed that the majority of the $VGLUT_2$-IR baskets did not coexpress either the cholinergic or noradrenergic marker, respectively. In fact, $VGLUT_2$- (Figs. 9A, E, I) and VAChT-LIs (Figs. 9B, F, J) were detected in different perineuronal baskets. However, in a few cases, $VGLUT_2$- (Figs. 9M) or VAChT-IR (Figs. 9N) varicosities innervating the same TH-IR MPG NP showed overlap (Figs. 9P).

Analysis of MPGs after its deafferentation showed that the occasional $VGLUT_1$-IR varicosities detected in contralateral PNA (Fig. 10A) or ipsilateral sham-PNA (Fig. 10C) disappear after PNA in the affected MPG (Fig. 10E). Accordingly, while abundant $VGLUT_2$-IR nerve fibers and several perineuronal baskets were observed in the contralateral PNA (Fig. 10B) or ipsilateral sham-PNA (Fig. 10D), the expression of $VGLUT_2$ was reduced to a few nerve fibers in the ipsilateral PNA (Fig. 10F). Neither $VGLUT_1$- or $VGLUT_2$-IR NPs were observed in MPGs after PNA (Fig. 10E, F) or SNA (data not shown). Riboprobe *in situ* hybridization of MPG sections in naïve mice failed to reveal signs of cellular expression of any of the studied VGLUT mRNAs (data not shown).

Discussion

In the present work, we show that axotomy of both visceral and non-visceral nerves induce the upregulation of $VGLUT_2$ protein and transcript in a subpopulation of LSC neurons. These observations suggest that some sympathetic neurons, upon direct injury of their postganglionic projections, can develop a glutamatergic phenotype. The presence of such a subpopulation of noradrenergic neurons in the LSC may seem surprising. However, coexpression of $VGLUT_2$ (Sulzer et al., 1998; Kawano et al., 2006; Yamaguchi et al., 2007) or glutamate (Liu et al., 1995; Sulzer et al., 1998) with TH, the latter a marker for dopaminergic neurons in this case, has been shown in rat (Sulzer et al., 1998; Stornetta et al., 2002a; Stornetta et al., 2002b; Kawano et al., 2006; Yamaguchi et al., 2007) and cat (Liu et al., 1995) brainstem, as well as in rat hypothalamus (Kawano et al., 2006). Interestingly,

expression and upregulation of $VGLUT_2$ in supraoptic and paraventricular neurons synthesizing vasopressin was also described in rats subjected to water deprivation (Kawasaki et al., 2005).

Postganglionic axotomy of sympathetic nerves in cat LSC (Lindh et al., 1993) or rodent SCG (Zhang et al., 1994; Zigmond and Sun 1997; Landry et al., 2000; Navarro et al., 2007) induces downregulation of neuropeptides such as CGRP (Lindh et al., 1993) and NPY, as well as the noradrenergic marker TH (Cheah and Geffen 1973; Sun and Zigmond 1996; Zigmond and Sun 1997; Landry et al., 2000; Navarro et al., 2007), and upregulation of galanin (Lindh et al., 1993; Zigmond and Sun 1997; Landry et al., 2000; Navarro et al., 2007), VIP, SP (Rao et al., 1993; Zigmond and Sun 1997; Landry et al., 2000; Navarro et al., 2007) and the NPY Y_2-receptor (Lindh et al., 1993; Zhang et al., 1994; Zigmond and Sun 1997; Landry et al., 2000; Navarro et al., 2007). More recently, in a study in pigs, it was shown that axotomy of the nerves innervating the colon and containing sympathetic fibers projecting from the LSC, results in the upregulation of galanin and to some extent somatostatin, paralleled by the downregulation of TH (Skobowiat et al., 2011). In the present study in mouse, we observed that PNA, a lesion that targets both sensory afferent as well as autonomic efferent nerves, induces upregulation of $VGLUT_2$ mRNA in about 7% of all LSC neurons, an event paralleled by the upregulation of $VGLUT_2$ protein. This lesion-induced plasticity was selective in that expression of $VGLUT_1$ and $VGLUT_3$ mRNAs was not induced.

Whether the upregulation of $VGLUT_2$ reflects induction (i.e., *de novo* synthesis of transporter protein and transcript) or an increase from low levels not detected with our methods is not known. The physiological consequences of such an event remain unknown, but $VGLUT_2$ upregulation in sympathetic neurons could result in increased synthesis, vesicular uptake and synaptic release of glutamate, from cell bodies or axonal projections, potentially contributing to increased fast synaptic transmission and nociceptive mechanisms. In fact, glutamate could be released from the soma of LSC neurons. There is abundant evidence supporting the concept of somatic/dendritic release for neuropeptides, monoamines and glutamate (Duguid et al., 2007; Colgan et al., 2009; Xia et al., 2009). Moreover, $VGLUT_2$ immunoreactivity can be observed close to the plasma membrane in non-visceral DRG cell bodies, suggesting somatic glutamate release (Brumovsky et al., 2007).

Because sensory neurons in rodents express VGLUTs/glutamate (Oliveira et al., 2003; Hwang et al., 2004; Landry et al., 2004; Morris et al., 2005; Brumovsky et al., 2007; Seal et al., 2009), glutamate acting on peripherally expressed glutamatergic receptors (see below) most likely derives from afferent fibers. However, and as suggested by our present findings, the axonal projections of LSC neurons could be an additional source of glutamate, participating in a process of sympathetic-sensory neuron coupling (Shinder et al., 1999; Habler et al., 2000; Janig 2003; Gibbs et al., 2008). It has been demonstrated that activation of peripheral glutamate receptors by exogenous glutamate (Carlton et al., 1995; Jackson et al., 1995; Du et al., 2001), NMDA (Du et al., 2003) or kainate (Du et al., 2006) receptor agonists in primary afferents present in the glabrous skin of the rat hindpaw induces their depolarization and promotes pain-related behavior; a similar effect was also observed in hairy skin (see (Tian et al., 2005)). Nevertheless, Moalem and colleagues (Moalem et al., 2005) reported that a number of chemical mediators including glutamate, did not affect the excitability of unmyelinated sensory axons in normal or injured peripheral nerves of the rat. Unfortunately, the potential role of glutamate and other chemical mediators on the excitability of thick and thinly myelinated fibers was not assessed in that study.

Evidence for glutamatergic signaling in autonomic neurons has previously been presented. In fact, application of kainate to peripheral noradrenergic ganglia innervating the rat vas

deferens was earlier shown to induce a time-dependent decrease of noradrenaline in this organ (Lara and Bastos-Ramos 1988). Moreover, NMDA receptor activation in isolated segments of the guinea pig colon potentiates the electrically stimulated noradrenaline overflow, a presynaptic effect probably exerted at sympathetic nerve terminals (Cosentino et al., 1995). In these studies, it was assumed that glutamate originated from sensory nerve terminals. However, our results on $VGLUT_2$ suggest that sympathetic neurons, at least after injury, may also contribute to peripherally released glutamate. Finally, supporting a role of glutamate in pain modulation, recent studies show that partial or total deletion of $VGLUT_2$ protein in primary afferent neurons markedly reduces sensory hypersensitivity induced by peripheral nerve lesions (Moechars et al., 2006; Leo et al., 2009; Liu et al., 2010; Lagerström et al., 2010). However, the expression of $VGLUT_2$ in the LSC of these mice, before and after injury, or the role of impairment of $VGLUT_2$ in the peripheral projections of DRG neurons were not assessed.

Expression of group I metabotropic (see (Shigemoto et al., 1992; Kammermeier and Ikeda 2002; Higashida et al., 2003)), as well as AMPA (Kiyama et al., 1993; Carlton et al., 1998; Coggeshall and Carlton 1999), NMDA (Carlton et al., 1998) (Coggeshall and Carlton 1999) and kainate (Coggeshall and Carlton 1999) ionotropic glutamate receptors in rodent superior cervical ganglion (SCG) (Shigemoto et al., 1992; Kiyama et al., 1993; Kammermeier and Ikeda 2002; Higashida et al., 2003) and LSC (Carlton et al., 1998; Coggeshall and Carlton 1999) neurons and their projections further supports a role of glutamate in the autonomic nervous system. Interestingly, Coggeshall and Carlton (Coggeshall and Carlton 1999) showed that the proportion of NMDA, AMPA and kainate receptors in the *gray rami* associated with the LSC in rat is considerably increased 48 hr after hindpaw inflammation. These glutamatergic receptors, under ‘normal’ circumstances presumably targeted by glutamate released from primary afferent nerve terminals could promote an augmented release of noradrenaline and other transmitters, potentially exacerbating the activation of sensory neurons in inflammatory states (Carlton et al., 1998; Coggeshall and Carlton 1999). Our results also suggest that autonomic neurons themselves could release glutamate, acting on primary afferent and/or autonomic nerve terminals, thus acting on hetero- or autoreceptors, or both. Also, enteric neurons in the gut or non-neuronal visceral tissues are putative targets of glutamate released by LSC nerve endings. It remains to be established whether inflammation of visceral organs or the hindpaw also induces $VGLUT_2$ upregulation in the LSC.

We also found that all NPs upregulating $VGLUT_2$-LI in the LSC coexpressed ATF-3, a transcription factor dramatically upregulated in lumbar DRG neurons in rodents after peripheral nerve injury (Tsujino et al., 2000). In addition, postganglionic axotomy of the superior cervical ganglion also upregulates ATF-3 in rat and mouse (Hyatt et al., 2007). Autonomic neurons, similar to sensory neurons, are characterized by their considerable capacity to survive and regenerate after peripheral nerve injury. Several molecules, including ATF-3 (see (Seijffers et al., 2007)), as well as classical ones like the nerve growth factor, have been proposed to be central to mechanisms of nerve regeneration (see (Keast 2006; Navarro et al., 2007)). Could the upregulation of $VGLUT_2$ and possibly also glutamate reflect a role in survival and regeneration of LSC neurons? (Balazs 2006). Interestingly, $VGLUT_2$- LI is present in neurons migrating from the olfactory placode toward the forebrain in the developing rat brain, gradually decreasing toward adulthood (Honma et al., 2004). Furthermore, an association between the expression of $VGLUT_2$ protein in mesencephalic dopaminergic axonal terminals and the formation of synaptic junctions by these terminals was recently reported, suggesting a role in axonal growth (Bérubé-Carriere et al., 2009). Classically, excessive activation of glutamatergic receptors has been linked to neurotoxicity (Mattson 2003). However, activation of different

metabotropic glutamate receptors in the central nervous system has also been shown to be neuroprotective (Byrnes et al., 2009).

Unexpectedly, we noted in sham mice, or the contralateral side of PNA mice, the existence of perineuronal baskets in MPGs expressing $VGLUT_2$ and lacking both TH and VAChT. These baskets appeared sparsely distributed throughout the ganglion, often but not exclusively around TH-IR MPG neurons. VAChT-IR baskets were also present in the ganglion, but were virtually always different than those expressing $VGLUT_2$, suggesting that these baskets may target different subpopulations of MPG neurons. Interestingly, deafferentation of the MPG by PNA induced a noticeable reduction in the number of $VGLUT_2$-IR nerve fibers, and abolished most of the $VGLUT_2$-IR baskets ipsilateral to the lesion, suggesting that these two structures are contributed by the pelvic nerve. Perineuronal baskets in the MPG have been described in rat (Keast 1995) and mouse (Wanigasekara et al., 2003). These are typically cholinergic, and often coexpress other transmitters, including neuropeptides (de Groat 1987; Wanigasekara et al., 2003; Keast 2006). Evidence of a glutamatergic trait in MPG perineuronal baskets has not been reported previously, with the exception of an electron microscopy study in rat showing glutamate in axons and terminals in the MPG, also containing large dense core vesicles (Aïoun and Rampin 2006). However, and possibly because of the nature of the experimental approach (electron microscopy), the authors did not assess the presence of perineuronal baskets containing glutamate in the MPG. The present results support the notion of expression of glutamate in nerve fibers innervating the MPG and also forming perineuronal baskets. Finally, in their study, Aïoun and Rampin also reported that the distribution and appearance of glutamatergic terminals in the MPG was similar to those of retrogradely traced penile sensory nerve terminals in this ganglion, targeting a specific subset of MPG neurons (Aïoun and Rampin 2006). Whether this is the case in our present work in mouse requires further investigation.

Thus, the origin of the $VGLUT_2$-IR baskets remains to be elucidated. They could derive from preganglionic autonomic spinal neurons. However, we found that the $VGLUT_2$-IR baskets did not coexpress VAChT, one of the standard immunohistochemical markers for identification of sympathetic or parasympathetic preganglionic neurons (Keast 2006). Alternatively, the baskets could arise from sensory DRG neurons (Lundberg et al., 1980; Matthews and Cuello 1984; Keast 2006). We explored this by co-staining for $VGLUT_2$ and CGRP, the latter often used as a marker for peptidergic sensory nerves due to its abundance in DRG neurons, and found that they virtually never coexist. However, only half of the $VGLUT_2$-IR neurons in lumbar (Brumovsky et al., 2007), thoracic and sacral DRGs (manuscript in preparation) coexpress CGRP. Therefore, the $VGLUT_2$-IR MPG baskets described here could be derived from non-peptidergic sensory fibers. Finally, the VAChT-positive baskets could have a sensory origin, since cholinergic DRG neurons have been described in the mouse (Bernardini et al., 2004; Tata et al., 2004).

Although less likely, two additional sources of $VGLUT_2$-IR baskets could be LSC or myenteric neurons. LSC neurons project their fibers, traversing the MPG, on their way to the target organs (Costa and Funess 1973; Hulsebosch and Coggeshall 1982; Kuo et al., 1984). Even though these neurons only seem to upregulate $VGLUT_2$ after nerve injury, they may normally express and transport peripherally very low levels of the transporter, accumulating in the terminals and becoming immunohistochemically detectable only at this location. Concerning myenteric neurons in the colorectum, we have recently discovered a very small subpopulation of these neurons in the mouse capable of expressing $VGLUT_2$ mRNA (unpublished data). Viscerofugal neurons terminating in the MPG have been described in the rat (Luckensmeyer and Keast 1995; Luckensmeyer and Keast 1996; Luckensmeyer and Keast 1998). Similar viscerofugal neurons have been described in mouse gut (Miller and Szurszewski 2002), although it remains to be established if they express $VGLUT_2$.

In conclusion, the present results highlight the possibility that glutamate may be upregulated and have a role in sympathetic neurons after injury. It remains to be established if this role could relate to pain, survival or regeneration mechanisms, or all functions. Furthermore, the presence of perineuronal baskets expressing $VGLUT_2$ of potential sensory origin in the mouse MPG supports the hypothesis of glutamatergic sensory-autonomic interactions.

Acknowledgments

We would like to thank Drs. Akiya Watakabe, National Institute for Basic Biology, Okazaki, Japan and Jeffery Erickson, Louisiana State University, New Orleans, LA, USA, for the generous donation of VGLUT *in situ* hybridization probes, and Dr. Kathy Albers, Pittsburgh Center for Pain Research, Department of Anesthesiology, University of Pittsburgh, PA, USA, for help with the preparation of the *in situ* hybridization probes. We also thank Mr. Tim McMurray for his excellent technical assistance. This study was supported by NIH awards NS19912 and NS 35790 to GFG, an IASP Early Career Research Award to PRB, an Austral University grant to PRB and the Swedish Research Council (04X-2287; TH).

References

1. Adams JC. Biotin amplification of biotin and horseradish peroxidase signals in histochemical stains. J. Histochem. Cytochem. 1992; 40:1457–1463. [PubMed: 1527370]
2. Aïoun J, Rampin O. Anatomical evidence for glutamatergic transmission in primary sensory neurons and onto postganglionic neurons controlling penile erection in rats: an ultrastructural study with neuronal tracing and immunocytochemistry. Cell. Tissue Res. 2006; 323:359–375. [PubMed: 16307288]
3. Apostolova G, Dechant G. Development of neurotransmitter phenotypes in sympathetic neurons. Auton. Neurosci. 2009; 151:30–38. [PubMed: 19734109]
4. Balazs R. Trophic effect of glutamate. Curr. Top. Med. Chem. 2006; 6:961–968. [PubMed: 16787270]
5. Bennett GJ, Xie YK. A peripheral mononeuropathy in rat that produces disorders of pain sensation like those seen in man. Pain. 1988; 33:87–107. [PubMed: 2837713]
6. Bernardini N, Tomassy GS, Tata AM, ugusti-Tocco G, Biagioni S. Detection of basal and potassium-evoked acetylcholine release from embryonic DRG explants. J. Neurochem. 2004; 88:1533–1539. [PubMed: 15009654]
7. Bérubé-Carriere N, Riad M, Dal BG, Lévesque D, Trudeau LE, Descarries L. The dual dopamine-glutamate phenotype of growing mesencephalic neurons regresses in mature rat brain. J. Comp. Neurol. 2009; 517:873–891. [PubMed: 19844994]
8. Brumovsky P, Watanabe M, Hökfelt T. Expression of the vesicular glutamate transporters-1 and -2 in adult mouse dorsal root ganglia and spinal cord and their regulation by nerve injury. Neuroscience. 2007; 147:469–490. [PubMed: 17577523]
9. Brumovsky PR, Bergman E, Liu HX, Hökfelt T, Villar MJ. Effect of a graded single constriction of the rat sciatic nerve on pain behavior and expression of immunoreactive NPY and NPY Y1 receptor in DRG neurons and spinal cord. Brain Res. 2004; 1006:87–99. [PubMed: 15047027]
10. Byrnes KR, Stoica B, Riccio A, Pajoohesh-Ganji A, Loane DJ, Faden AI. Activation of metabotropic glutamate receptor 5 improves. Ann. Neurol. 2009; 66:63–74. [PubMed: 19670441]
11. Carlton SM, Chung K, Ding Z, Coggeshall RE. Glutamate receptors on postganglionic sympathetic axons. Neuroscience. 1998; 83:601–605. [PubMed: 9460766]
12. Carlton SM, Hargett GL, Coggeshall RE. Localization and activation of glutamate receptors in unmyelinated axons of rat glabrous skin. Neurosci. Lett. 1995; 197:25–28. [PubMed: 8545047]
13. Cheah TB, Geffen LB. Effects of axonal injury on norepinephrine, tyrosine hydroxylase and monoamine oxidase levels in sympathetic ganglia. J. Neurobiol. 1973; 4:443–452. [PubMed: 4147762]
14. Coggeshall RE, Carlton SM. Evidence for an inflammation-induced change in the local glutamatergic regulation of postganglionic sympathetic efferents. Pain. 1999; 83:163–168. [PubMed: 10534587]

15. Colgan LA, Putzier I, Levitan ES. Activity-dependent vesicular monoamine transporter-mediated depletion of the nucleus supports somatic release by serotonin neurons. J. Neurosci. 2009; 29:15878–15887. [PubMed: 20016104]

16. Coons AH. Fluorescent antibody methods. Gen. Cytochem. Meth. 1958; 1:399–422.

17. Cosentino M, De PF, Marino F, Giaroni C, Leoni O, Lecchini S, Frigo G. N-methyl-D-aspartate receptors modulate neurotransmitter release and peristalsis in the guinea pig isolated colon. Neurosci. Lett. 1995; 183:139–142. [PubMed: 7746475]

18. Costa M, Funess JB. Observations on the anatomy and amine histochemistry of the nerves and ganglia which supply the pelvic viscera and on the associated chromaffin tissue in the guinea-pig. Z. Anat. Entwicklungsgesch. 1973; 140:85–108. [PubMed: 4749133]

19. Costigan M, Befort K, Karchewski L, Griffin RS, D'Urso D, Allchorne A, Sitarski J, Mannion JW, Pratt RE, Woolf CJ. Replicate high-density rat genome oligonucleotide microarrays reveal hundreds of regulated genes in the dorsal root ganglion after peripheral nerve injury. BMC Neurosci. 2002; 3:16. [PubMed: 12401135]

20. de Groat WC. Neuropeptides in pelvic afferent pathways. Experientia. 1987; 43:801–813. [PubMed: 3297768]

21. Dickerson JW, Hemmerle AM, Numan S, Lundgren KH, Seroogy KB. Decreased expression of ErbB4 and tyrosine hydroxylase mRNA and protein in the ventral midbrain of aged rats. Neuroscience. 2009; 163:482–489. [PubMed: 19505538]

22. Du J, Koltzenburg M, Carlton SM. Glutamate-induced excitation and sensitization of nociceptors in rat glabrous skin. Pain. 2001; 89:187–198. [PubMed: 11166475]

23. Du J, Zhou S, Carlton SM. Kainate-induced excitation and sensitization of nociceptors in normal and inflamed rat glabrous skin. Neuroscience. 2006; 137:999–1013. [PubMed: 16330152]

24. Du J, Zhou S, Coggeshall RE, Carlton SM. N-methyl-D-aspartate-induced excitation and sensitization of normal and inflamed nociceptors. Neuroscience. 2003; 118:547–562. [PubMed: 12699789]

25. Duguid IC, Pankratov Y, Moss GW, Smart TG. Somatodendritic release of glutamate regulates synaptic inhibition in cerebellar Purkinje cells via autocrine mGluR1 activation. J. Neurosci. 2007; 27:12464–12474. [PubMed: 18003824]

26. Elfvin LG, Lindh B, Hökfelt T. The chemical neuroanatomy of sympathetic ganglia. Annu. Rev. Neurosci. 1993; 16:471–507. [PubMed: 8384808]

27. Fremeau RT Jr, Voglmaier S, Seal RP, Edwards RH. VGLUTs define subsets of excitatory neurons and suggest novel roles for glutamate. Trends Neurosci. 2004; 27:98–103. [PubMed: 15102489]

28. Furness JB. The organisation of the autonomic nervous system: peripheral connections. Auton. Neurosci. 2006; 130:1–5. [PubMed: 16798102]

29. Furness JB, Jones C, Nurgali K, Clerc N. Intrinsic primary afferent neurons and nerve circuits within the intestine. Prog. Neurobiol. 2004; 72:143–164. [PubMed: 15063530]

30. Gibbs GF, Drummond PD, Finch PM, Phillips JK. Unravelling the pathophysiology of complex regional pain syndrome: focus on sympathetically maintained pain. Clin. Exp. Pharmacol. Physiol. 2008; 35:717–724. [PubMed: 18215185]

31. Habler H, Eschenfelder S, Liu XG, Jänig W. Sympathetic-sensory coupling after L5 spinal nerve lesion in the rat and its relation to changes in dorsal root ganglion blood flow. Pain. 2000; 87:335–345. [PubMed: 10963913]

32. Higashida H, Zhang JS, Mochida S, Chen XL, Shin Y, Noda M, Hossain KZ, Hoshi N, Hashii M, Shigemoto R, Nakanishi S, Fukuda Y, Yokoyama S. Subtype-specific coupling with ADP-ribosyl cyclase of metabotropic glutamate receptors in retina, cervical superior ganglion and NG108-15 cells. J. Neurochem. 2003; 85:1148–1158. [PubMed: 12753074]

33. Honma S, Kawano M, Hayashi S, Kawano H, Hisano S. Expression and immunohistochemical localization of vesicular glutamate transporter 2 in the migratory pathway from the rat olfactory placode. Eur. J. Neurosci. 2004; 20:923–936. [PubMed: 15305861]

34. Hughes DI, Polgar E, Shehab SA, Todd AJ. Peripheral axotomy induces depletion of the vesicular glutamate transporter VGLUT1 in central terminals of myelinated afferent fibres in the rat spinal cord. Brain Res. 2004; 1017:69–76. [PubMed: 15261101]

35. Hulsebosch CE, Coggeshall RE. An analysis of the axon populations in the nerves to the pelvic viscera in the rat. J. Comp. Neurol. 1982; 211:1–10. [PubMed: 7174880]
36. Hwang SJ, Burette A, Rustioni A, Valtschanoff JG. Vanilloid receptor VR1-positive primary afferents are glutamatergic and contact spinal neurons that co-express neurokinin receptor NK1 and glutamate receptors. J. Neurocytol. 2004; 33:321–329. [PubMed: 15475687]
37. Hyatt SH, Schreiber RC, Shoemaker SE, Sabe A, Reed E, Zigmond RE. Activating transcription factor 3 induction in sympathetic neurons after axotomy: response to decreased neurotrophin availability. Neuroscience. 2007; 150:887–897. [PubMed: 18031939]
38. Jackson DL, Graff CB, Richardson JD, Hargreaves KM. Glutamate participates in the peripheral modulation of thermal hyperalgesia in rats. Eur. J. Pharmacol. 1995; 284:321–325. [PubMed: 8666015]
39. Jaggi AS, Jain V, Singh N. Animal models of neuropathic pain. Fundam. Clin. Pharmacol. 2011; 25:1–28. [PubMed: 20030738]
40. Jänig W. Relationship between pain and autonomic phenomena in headache and other pain conditions. Cephalalgia. 2003; 23 Suppl 1:43–48.
41. Kammermeier PJ, Ikeda SR. Metabotropic glutamate receptor expression in the rat superior cervical ganglion. Neurosci. Lett. 2002; 330:260–264. [PubMed: 12270642]
42. Kaneko T, Fujiyama F. Complementary distribution of vesicular glutamate transporters in the central nervous system. Neurosci. Res. 2002; 42:243–250. [PubMed: 11985876]
43. Kawamura Y, Fukaya M, Maejima T, Yoshida T, Miura E, Watanabe M, Ohno-Shosaku T, Kano M. The CB1 cannabinoid receptor is the major cannabinoid receptor at excitatory presynaptic sites in the hippocampus and cerebellum. J. Neurosci. 2006; 26:2991–3001. [PubMed: 16540577]
44. Kawano M, Kawasaki A, Sakata-Haga H, Fukui Y, Kawano H, Nogami H, Hisano S. Particular subpopulations of midbrain and hypothalamic dopamine neurons express vesicular glutamate transporter 2 in the rat brain. J. Comp. Neurol. 2006; 498:581–592. [PubMed: 16917821]
45. Kawasaki A, Hoshi K, Kawano M, Nogami H, Yoshikawa H, Hisano S. Up-regulation of VGLUT2 expression in hypothalamic-neurohypophysial neurons of the rat following osmotic challenge. Eur. J. Neurosci. 2005; 22:672–680. [PubMed: 16101749]
46. Keast JR. Plasticity of pelvic autonomic ganglia and urogenital innervation. Int. Rev. Cytol. 2006; 248:141–208. [PubMed: 16487791]
47. Keast JR. Visualization and immunohistochemical characterization of sympathetic and parasympathetic neurons in the male rat major pelvic ganglion. Neuroscience. 1995; 66:655–662. [PubMed: 7644029]
48. Kiyama H, Sato K, Kuba T, Tohyama M. Sympathetic and parasympathetic ganglia express non-NMDA type glutamate receptors: distinct receptor subunit composition in the principle and SIF cells. Brain Res. Mol. Brain Res. 1993; 19:345–348. [PubMed: 8231738]
49. Kubista M, Akerman B, Norden B. Characterization of interaction between DNA and 4',6-diamidino-2-phenylindole by optical spectroscopy. Biochemistry. 1987; 26:4545–4553. [PubMed: 3663606]
50. Kuo DC, Hisamitsu T, de Groat WC. A sympathetic projection from sacral paravertebral ganglia to the pelvic nerve and to postganglionic nerves on the surface of the urinary bladder and large intestine of the cat. J. Comp. Neurol. 1984; 226:76–86. [PubMed: 6736296]
51. Lagerström MC, Rogoz K, Abrahamsen B, Persson E, Reinius B, Nordenankar K, Olund C, Smith C, Mendez JA, Chen ZF, Wood JN, Wallen-Mackenzie A, Kullander K. VGLUT2-dependent sensory neurons in the TRPV1 population regulate pain and itch. Neuron. 2010; 68:529–542. [PubMed: 21040852]
52. Landry M, Bouali-Benazzouz R, El MS, Ravassard P, Nagy F. Expression of vesicular glutamate transporters in rat lumbar spinal cord, with a note on dorsal root ganglia. J. Comp. Neurol. 2004; 468:380–394. [PubMed: 14681932]
53. Landry M, Holmberg K, Zhang X, Hökfelt T. Effect of axotomy on expression of NPY, galanin, and NPY Y1 and Y2 receptors in dorsal root ganglia and the superior cervical ganglion studied with double-labeling in situ hybridization and immunohistochemistry. Exp. Neurol. 2000; 162:361–384. [PubMed: 10739642]

54. Lara H, Bastos-Ramos W. Glutamate and kainate effects on the noradrenergic neurons innervating the rat vas deferens. J. Neurosci. Res. 1988; 19:239–244. [PubMed: 2896801]
55. Lein ES, Hawrylycz MJ, Ao N, Ayres M, Bensinger A, Bernard A, Boe AF, Boguski MS, Brockway KS, Byrnes EJ, Chen L, Chen L, Chen TM, Chin MC, Chong J, Crook BE, Czaplinska A, Dang CN, Datta S, Dee NR, Desaki AL, Desta T, Diep E, Dolbeare TA, Donelan MJ, Dong HW, Dougherty JG, Duncan BJ, Ebbert AJ, Eichele G, Estin LK, Faber C, Facer BA, Fields R, Fischer SR, Fliss TP, Frensley C, Gates SN, Glattfelder KJ, Halverson KR, Hart MR, Hohmann JG, Howell MP, Jeung DP, Johnson RA, Karr PT, Kawal R, Kidney JM, Knapik RH, Kuan CL, Lake JH, Laramee AR, Larsen KD, Lau C, Lemon TA, Liang AJ, Liu Y, Luong LT, Michaels J, Morgan JJ, Morgan RJ, Mortrud MT, Mosqueda NF, Ng LL, Ng R, Orta GJ, Overly CC, Pak TH, Parry SE, Pathak SD, Pearson OC, Puchalski RB, Riley ZL, Rockett HR, Rowland SA, Royall JJ, Ruiz MJ, Sarno NR, Schaffnit K, Shapovalova NV, Sivisay T, Slaughterbeck CR, Smith SC, Smith KA, Smith BI, Sodt AJ, Stewart NN, Stumpf KR, Sunkin SM, Sutram M, Tam A, Teemer CD, Thaller C, Thompson CL, Varnam LR, Visel A, Whitlock RM, Wohnoutka PE, Wolkey CK, Wong VY, Wood M, Yaylaoglu MB, Young RC, Youngstrom BL, Yuan XF, Zhang B, Zwingman TA, Jones AR. Genome-wide atlas of gene expression in the adult mouse brain. Nature. 2007; 445:168–176. [PubMed: 17151600]
56. Leo S, Moechars D, Callaerts-Vegh Z, D'Hooge R, Meert T. Impairment of VGLUT2 but not VGLUT1 signaling reduces neuropathy-induced hypersensitivity. Eur. J. Pain. 2009; 13:1008–1017. [PubMed: 19171494]
57. Liguz-Lecznar M, Skangiel-Kramska J. Vesicular glutamate transporters (VGLUTs): the three musketeers of glutamatergic system. Acta Neurobiol. Exp. (Wars.). 2007; 67:207–218. [PubMed: 17957901]
58. Lindh B, Risling M, Remahl S, Terenius L, Hökfelt T. Peptide-immunoreactive neurons and nerve fibres in lumbosacral sympathetic ganglia: selective elimination of a pathway-specific expression of immunoreactivities following sciatic nerve resection in kittens. Neuroscience. 1993; 55:545–562. [PubMed: 7690913]
59. Liu RH, Fung SJ, Reddy VK, Barnes CD. Localization of glutamatergic neurons in the dorsolateral pontine tegmentum projecting to the spinal cord of the cat with a proposed role of glutamate on lumbar motoneuron activity. Neuroscience. 1995; 64:193–208. [PubMed: 7708205]
60. Liu Y, Abdel SO, Zhang L, Duan B, Tong Q, Lopes C, Ji RR, Lowell BB, Ma Q. VGLUT2-dependent glutamate release from nociceptors is required to sense pain and suppress itch. Neuron. 2010; 68:543–556. [PubMed: 21040853]
61. Luckensmeyer GB, Keast JR. Distribution and morphological characterization of viscerofugal projections from the large intestine to the inferior mesenteric and pelvic ganglia of the male rat. Neuroscience. 1995; 66:663–671. [PubMed: 7543983]
62. Luckensmeyer GB, Keast JR. Immunohistochemical characterisation of viscerofugal neurons projecting to the inferior mesenteric and major pelvic ganglia in the male rat. J. Auton. Nerv. Syst. 1996; 61:6–16. [PubMed: 8912248]
63. Luckensmeyer GB, Keast JR. Characterisation of the adventitial rectal ganglia in the male rat by their immunohistochemical features and projections. J. Comp. Neurol. 1998; 396:429–441. [PubMed: 9651003]
64. Lundberg, JM.; Hökfelt, T.; Anggard, A.; Uvnas-Wallensten, K.; Brimijoin, S.; Brodin, E.; Fahrenkrug, J. Peripheral peptide neurons: Distribution, axonal transport, and some aspects on possible function. In: Costa, E.; Trabucchi, M., editors. Neural Peptides and Neuronal Communication. New York: Raven Press; 1980. p. 25-36.
65. Matthews MR, Cuello AC. The origin and possible significance of substance P immunoreactive networks in the prevertebral ganglia and related structures in the guinea-pig. Philos. Trans. R. Soc. Lond. B. Biol. Sci. 1984; 306:247–276. [PubMed: 6207550]
66. Mattson MP. Excitotoxic and excitoprotective mechanisms: abundant targets for the prevention and treatment of neurodegenerative disorders. Neuromol. Med. 2003; 3:65–94.
67. Miller SM, Szurszewski JH. Relationship between colonic motility and cholinergic mechanosensory afferent synaptic input to mouse superior mesenteric ganglion. Neurogastroenterol. Motil. 2002; 14:339–348. [PubMed: 12213101]

68. Miura E, Fukaya M, Sato T, Sugihara K, Asano M, Yoshioka K, Watanabe M. Expression and distribution of JNK/SAPK-associated scaffold protein JSAP1 in developing and adult mouse brain. J. Neurochem. 2006; 97:1431–1446. [PubMed: 16606357]
69. Miyazaki T, Fukaya M, Shimizu H, Watanabe M. Subtype switching of vesicular glutamate transporters at parallel fibre-Purkinje cell synapses in developing mouse cerebellum. Eur. J. Neurosci. 2003; 17:2563–2572. [PubMed: 12823463]
70. Moalem G, Grafe P, Tracey DJ. Chemical mediators enhance the excitability of unmyelinated sensory axons in normal and injured peripheral nerve of the rat. Neuroscience. 2005; 134:1399–1411. [PubMed: 16039795]
71. Moechars D, Weston MC, Leo S, Callaerts-Vegh Z, Goris I, Daneels G, Buist A, Cik M, van der SP, Kass S, Meert T, D'Hooge R, Rosenmund C, Hampson RM. Vesicular glutamate transporter VGLUT2 expression levels control quantal size and neuropathic pain. J. Neurosci. 2006; 26:12055–12066. [PubMed: 17108179]
72. Morris JL, Konig P, Shimizu T, Jobling P, Gibbins IL. Most peptide-containing sensory neurons lack proteins for exocytotic release and vesicular transport of glutamate. J. Comp. Neurol. 2005; 483:1–16. [PubMed: 15672399]
73. Nakamura K, Watakabe A, Hioki H, Fujiyama F, Tanaka Y, Yamamori T, Kaneko T. Transiently increased colocalization of vesicular glutamate transporters 1 and 2 at single axon terminals during postnatal development of mouse neocortex: a quantitative analysis with correlation coefficient. Eur. J. Neurosci. 2007; 26:3054–3067. [PubMed: 18028110]
74. Navarro X, Vivo M, Valero-Cabre A. Neural plasticity after peripheral nerve injury and regeneration. Prog. Neurobiol. 2007; 82:163–201. [PubMed: 17643733]
75. Ng L, Bernard A, Lau C, Overly CC, Dong HW, Kuan C, Pathak S, Sunkin SM, Dang C, Bohland JW, Bokil H, Mitra PP, Puelles L, Hohmann J, Anderson DJ, Lein ES, Jones AR, Hawrylycz M. An anatomic gene expression atlas of the adult mouse brain. Nat. Neurosci. 2009; 12:356–362. [PubMed: 19219037]
76. Numan S, Gall CM, Seroogy KB. Developmental expression of neurotrophins and their receptors in postnatal rat ventral midbrain. J. Mol. Neurosci. 2005; 27:245–260. [PubMed: 16186635]
77. Oliveira AL, Hydling F, Olsson E, Shi T, Edwards RH, Fujiyama F, Kaneko T, Hökfelt T, Cullheim S, Meister B. Cellular localization of three vesicular glutamate transporter mRNAs and proteins in rat spinal cord and dorsal root ganglia. Synapse. 2003; 50:117–129. [PubMed: 12923814]
78. Olsson C, Costa M, Brookes SJ. Neurochemical characterization of extrinsic innervation of the guinea pig rectum. J. Comp. Neurol. 2004; 470:357–371. [PubMed: 14961562]
79. Rao MS, Sun Y, Vaidyanathan U, Landis SC, Zigmond RE. Regulation of substance P is similar to that of vasoactive intestinal peptide after axotomy or explantation of the rat superior cervical ganglion. J. Neurobiol. 1993; 24:571–580. [PubMed: 7686961]
80. Robinson DR, Gebhart GF. Inside information: the unique features of visceral sensation. Mol. Interv. 2008; 8:242–253. [PubMed: 19015388]
81. Schäfer MK, Varoqui H, Defamie N, Weihe E, Erickson JD. Molecular cloning and functional identification of mouse vesicular glutamate transporter 3 and its expression in subsets of novel excitatory neurons. J. Biol. Chem. 2002; 277:50734–50748. [PubMed: 12384506]
82. Seal RP, Wang X, Guan Y, Raja SN, Woodbury CJ, Basbaum AI, Edwards RH. Injury-induced mechanical hypersensitivity requires C-low threshold mechanoreceptors. Nature. 2009; 462:651–655. [PubMed: 19915548]
83. Seijffers R, Mills CD, Woolf CJ. ATF3 increases the intrinsic growth state of DRG neurons to enhance peripheral nerve regeneration. J. Neurosci. 2007; 27:7911–7920. [PubMed: 17652582]
84. Seroogy, KB.; Herman, JP. *In situ* hybridization approaches to the study of the nervous system. In: Turner, AJ.; Bachelard, HS., editors. Neurochemistry—a practical approach. Oxford: Oxford University Press; 1997. p. 121-150.
85. Shigemoto R, Ohishi H, Nakanishi S, Mizuno N. Expression of the mRNA for the rat NMDA receptor (NMDAR1) in the sensory and autonomic ganglion neurons. Neurosci. Lett. 1992; 144:229–232. [PubMed: 1436707]

86. Shinder V, Govrin-Lippmann R, Cohen S, Belenky M, Ilin P, Fried K, Wilkinson HA, Devor M. Structural basis of sympathetic-sensory coupling in rat and human dorsal root ganglia following peripheral nerve injury. J. Neurocytol. 1999; 28:743–761. [PubMed: 10859576]

87. Skobowiat C, Calka J, Majewski M. Axotomy induced changes in neuronal plasticity of sympathetic chain ganglia (SChG) neurons supplying descending colon in the pig. Exp. Mol. Pathol. 2011; 90:13–18. [PubMed: 21110956]

88. Spencer NJ, Kerrin A, Singer CA, Hennig GW, Gerthoffer WT, McDonnell O. Identification of capsaicin-sensitive rectal mechanoreceptors activated by rectal distension in mice. Neuroscience. 2008; 153:518–534. [PubMed: 18395992]

89. Stornetta RL, Sevigny CP, Guyenet PG. Vesicular glutamate transporter DNPI/VGLUT2 mRNA is present in C1 and several other groups of brainstem catecholaminergic neurons. J. Comp. Neurol. 2002a; 444:191–206. [PubMed: 11840474]

90. Stornetta RL, Sevigny CP, Schreihofer AM, Rosin DL, Guyenet PG. Vesicular glutamate transporter DNPI/VGLUT2 is expressed by both C1 adrenergic and nonaminergic presympathetic vasomotor neurons of the rat medulla. J. Comp. Neurol. 2002b; 444:207–220. [PubMed: 11840475]

91. Sulzer D, Joyce MP, Lin L, Geldwert D, Haber SN, Hattori T, Rayport S. Dopamine neurons make glutamatergic synapses in vitro. J. Neurosci. 1998; 18:4588–4602. [PubMed: 9614234]

92. Sun Y, Zigmond RE. Involvement of leukemia inhibitory factor in the increases in galanin and vasoactive intestinal peptide mRNA and the decreases in neuropeptide Y and tyrosine hydroxylase mRNA in sympathetic neurons after axotomy. J. Neurochem. 1996; 67:1751–1760. [PubMed: 8858962]

93. Tata AM, De Stefano ME, Srubek TG, Vilaro MT, Levey AI, Biagioni S. Subpopulations of rat dorsal root ganglion neurons express active vesicular acetylcholine transporter. J. Neurosci. Res. 2004; 75:194–202. [PubMed: 14705140]

94. Tian YL, Guo Y, Cao DY, Zhang Q, Wang HS, Zhao Y. Local application of morphine suppresses glutamate-evoked activities of C and Adelta afferent fibers in rat hairy skin. Brain Res. 2005; 1059:28–34. [PubMed: 16168967]

95. Tsujino H, Kondo E, Fukuoka T, Dai Y, Tokunaga A, Miki K, Yonenobu K, Ochi T, Noguchi K. Activating transcription factor 3 (ATF3) induction by axotomy in sensory and motoneurons: A novel neuronal marker of nerve injury. Mol. Cell. Neurosci. 2000; 15:170–182. [PubMed: 10673325]

96. Wall PD, Devor M, Inbal R, Scadding JW, Schonfeld D, Seltzer Z, Tomkiewicz MM. Autotomy following peripheral nerve lesions: experimental anaesthesia dolorosa. Pain. 1979; 7:103–111. [PubMed: 574931]

97. Wanigasekara Y, Kepper ME, Keast JR. Immunohistochemical characterisation of pelvic autonomic ganglia in male mice. Cell Tissue Res. 2003; 311:175–185. [PubMed: 12596037]

98. Xia X, Lessmann V, Martin TF. Imaging of evoked dense-core-vesicle exocytosis in hippocampal neurons reveals long latencies and kiss-and-run fusion events. J. Cell Sci. 2009; 122:75–82. [PubMed: 19066284]

99. Xiao HS, Huang QH, Zhang FX, Bao L, Lu YJ, Guo C, Yang L, Huang WJ, Fu G, Xu SH, Cheng XP, Yan Q, Zhu ZD, Zhang X, Chen Z, Han ZG, Zhang X. Identification of gene expression profile of dorsal root ganglion in the rat peripheral axotomy model of neuropathic pain. Proc. Natl. Acad. Sci. U S A. 2002; 99:8360–8365. [PubMed: 12060780]

100. Yamaguchi T, Sheen W, Morales M. Glutamatergic neurons are present in the rat ventral tegmental area. Eur. J. Neurosci. 2007; 25:106–118. [PubMed: 17241272]

101. Zamboni I, De Martino C. Buffered picric acid formaldehyde. A new rapid fixative for electron microscopy. J. Cell Biol. 1967; 35:148A.

102. Zhang X, Dagerlind A, Bao L, Ji RR, Lundberg JM, Hökfelt T. Increased expression of galanin in the rat superior cervical ganglion after pre- and postganglionic nerve lesions. Exp. Neurol. 1994; 127:9–22. [PubMed: 7515354]

103. Zigmond RE, Sun Y. Regulation of neuropeptide expression in sympathetic neurons. Paracrine and retrograde influences. Ann. N. Y. Acad. Sci. 1997; 814:181–197. [PubMed: 9160971]

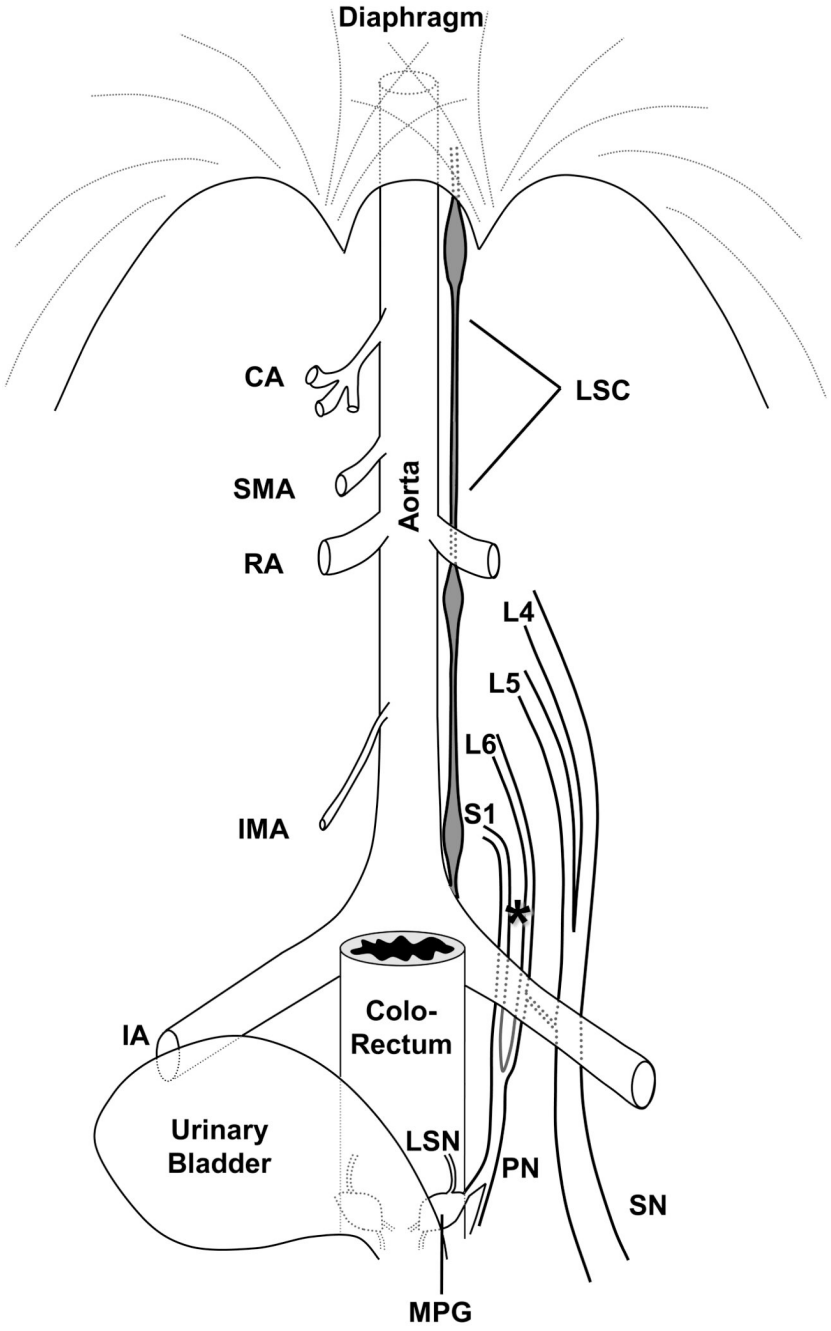

Figure 1.

Schematic diagram showing the general anatomical distribution of the lumbar sympathetic chain (LSC), the ventral branches of the spinal nerves L4-L6 and S1, the major pelvic ganglion (MPG), and the pelvic (PN), lumbar splanchnic (LSN) and sciatic (SN) nerves in the male mouse. Their relation with the aorta and stemming branches (celiac artery (CA), superior mesenteric artery (SMA), renal artery (RA), inferior mesenteric artery (IMA), iliac artery (IA)) is emphasized. Not illustrated for clarity is the spine, spinal cord or dorsal root ganglia, from which the axons of the spinal nerves arise. The nerves were exposed by blunt dissection of the overlying lumbar muscles (not shown); the location where transection of the pelvic nerve tributaries was executed is shown with an asterisk. The MPG is located

between the colorectum and the urinary bladder, with branches from the pelvic nerve traveling through it (for clarity, other branches entering or exiting the MPG are not illustrated).

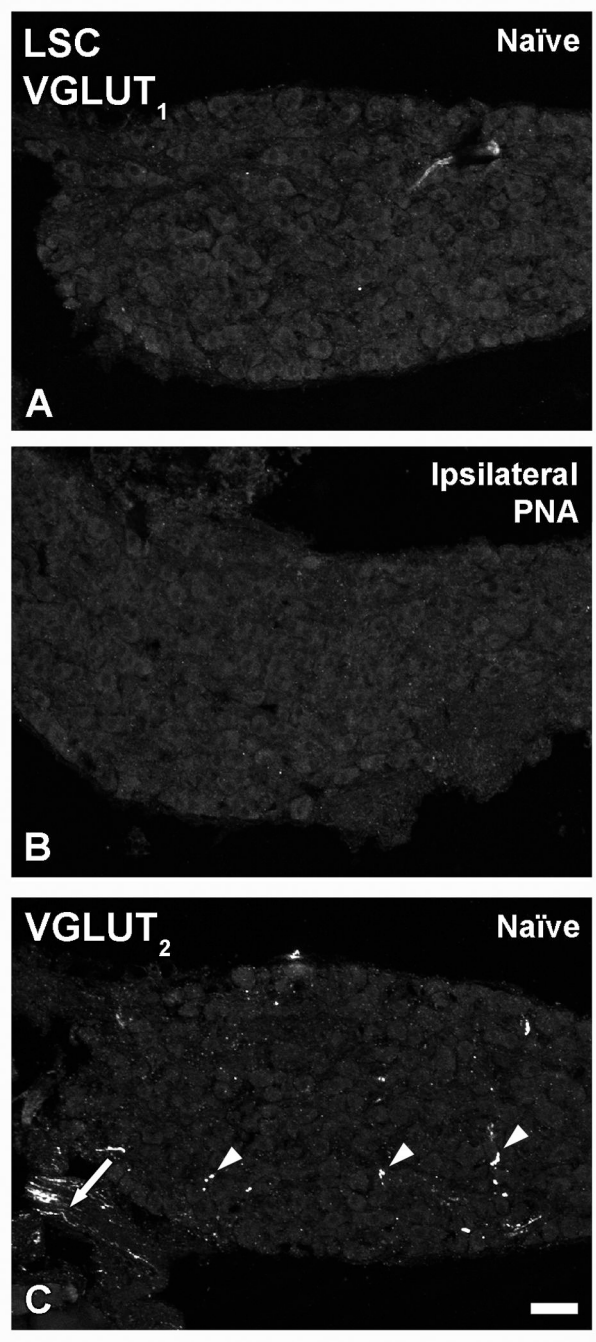

Figure 2.
Confocal immunofluorescence photomicrographs of sections of the LSC from naïve mice (A, C) or PNA mice (B), incubated with $VGLUT_1$ (A, B) or $VGLUT_2$ (C) antisera. Arrowheads and arrow in (C) show $VGLUT_2$-IR varicosities and nerve fibers, respectively in naïve LSCs. Scale bar: 50 μm.

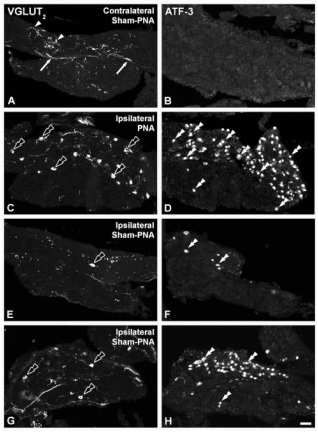

Figure 3.

Confocal immunofluorescence photomicrographs of sections of the contralateral (A, B) or ipsilateral (C–H) LSC of mice 7 days after sham-PNA (A,B; E–H) or PNA (C, D), incubated with $VGLUT_2$ (A, C, E, G) or ATF-3 (B, D, F, H) antisera (each corresponding pair of $VGLUT_2$ or ATF-3 micrographs shows sections separated by 36 μm). Arrows and arrowheads in (A, B) show $VGLUT_2$-IR fibers and varicosities, respectively. Black double arrowheads and double arrowheads in (C, D, E–H) show $VGLUT_2$- and ATF-3-IR LSC NPs. Scale bar: 50 μm (H=A–G).

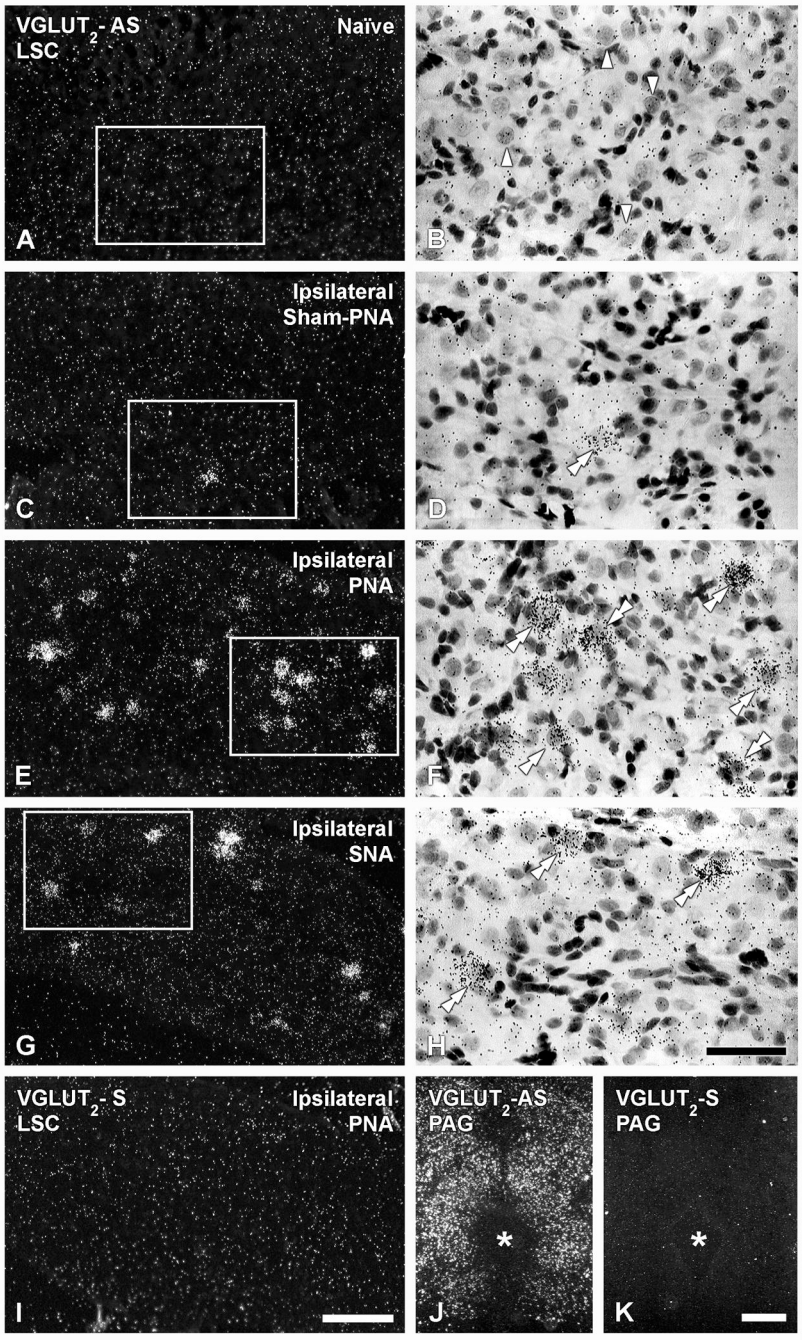

Figure 4.

Dark-(A, C, E, G, I, J, K) and bright-field (B, D, F, H) photomicrographs of LSC (A–H; I) or the PAG (J, K), in naïve (A, B, J, K), ipsilateral sham-PNA (C, D), ipsilateral PNA (E, F, I) or ipsilateral SNA (G, H), after hybridization with antisense (A–H; J) and sense (I, K) riboprobes for $VGLUT_2$ mRNA (B, D, F and H show high power magnification images of boxes in A, C, E and G, respectively). (Arrowheads in B show NPs lacking $VGLUT_2$ mRNA. Double arrowheads in D, F, H show $VGLUT_2$ mRNA-expressing NPs. Asterisk shows location of the aqueduct of Sylvius. Scale bars: 50 μm (H=B, D, F); 100 μm (I=A, C, E, G); 500 μm (J, K).

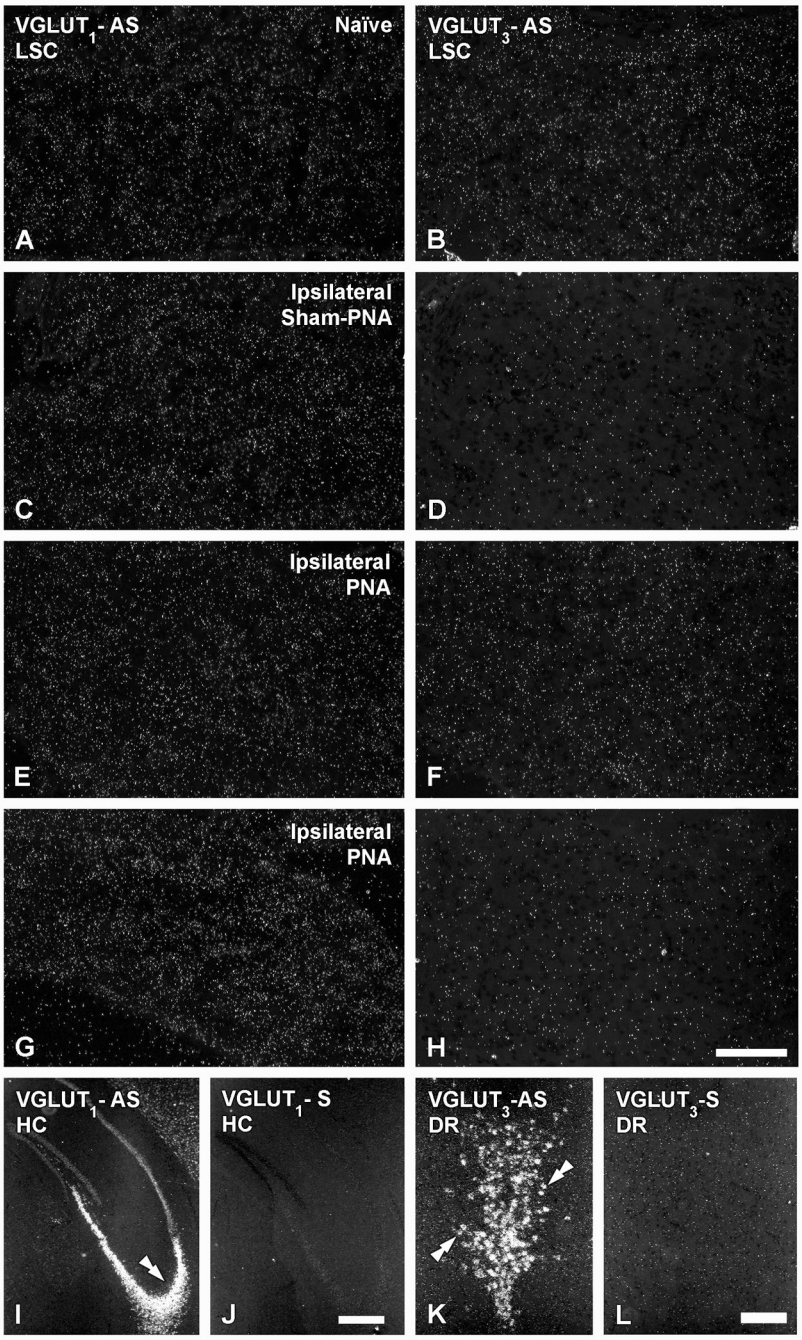

Figure 5.

Dark-field photomicrographs of LSC (A–H), the hippocampus (HC) (I, J) or the dorsal raphe nucleus (DR) (K, L), in naïve (A, B, I–L), ipsilateral sham-PNA (C, D), ipsilateral PNA (E, F) or ipsilateral SNA (G, H), after hybridization with antisense (A–H; I, K) and sense (J, L) riboprobes for $VGLUT_1$ (A, C, E, G, I, J) or $VGLUT_3$ (B, D, F, H, K, L) mRNAs. Double arrow in (I) and double arrows in (K) show mRNA labeling in the CA3 region of the HC or the DR, respectively. Scale bars: 50 μm (H=A–G); 200 μm (K, L); 500 μm (I, J).

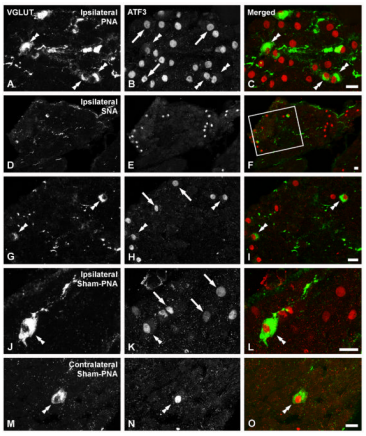

Figure 6.

Confocal immunofluorescence photomicrographs of sections of the ipsilateral LSC of mice 7 days after PNA (A–C), 10 days after SNA (D–I), ipsilateral (J–L) or contralateral to a sham-PNA (M–O), incubated with $VGLUT_2$ (A, D, G, J, M) and ATF-3 (B, E, H, K, N) antisera (C, F, I, L, O show merged images). (D–I; G–H show a magnified view of the box in F). Double arrowheads in (A, G, J, M, B, H, K, N, C, I, L, O) and arrows in (B, H, K) show VGLUT2/ATF-3 or ATF-3-only neurons, respectively. Scale bars: 20 μm (C=A, B; F=D, E; I=G, H; L=J, K; O=M, N).

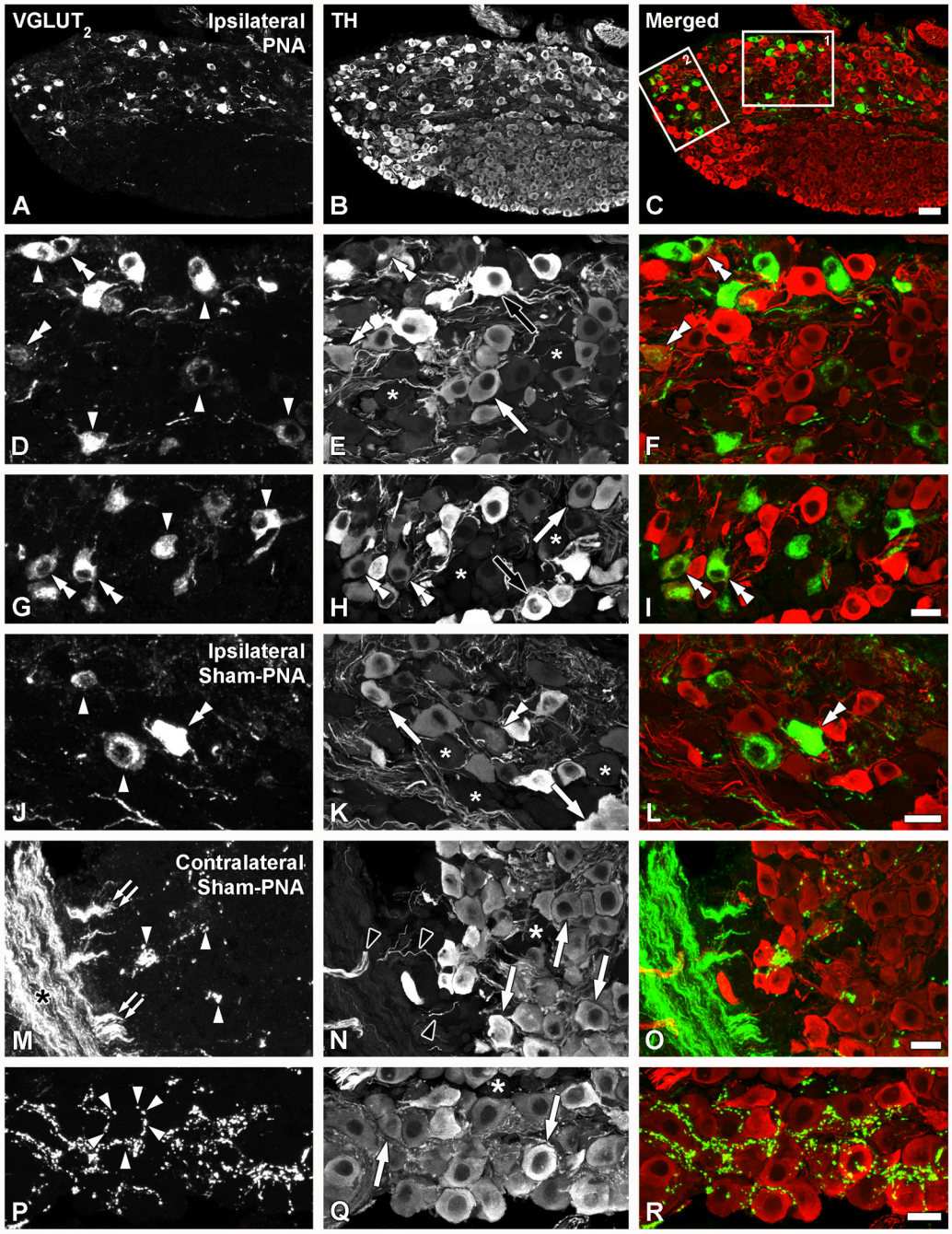

Figure 7.

Confocal immunofluorescence photomicrographs of sections of the ipsilateral (A–L) or contralateral (M–R) LSCs of mice 7 days after PNA (A–I) or sham-PNA (J–R), incubated with $VGLUT_2$ (A, D, G, J, M, P) and TH (B, E, H, K, N, Q) antisera (C, F, I, L, O, R show merged images) (asterisks in E, H, K, N, Q indicate TH-negative LSC NPs). (A–I; boxes 1 and 2 in C are shown at higher magnification in D–F and G–I, respectively). Arrowheads in (D, G, J) and double arrowheads in (D, G, J, B, H, K, F, I, L) show TH-only or $VGLUT_2$/TH neurons, respectively. White arrows and black arrows show light or strong TH-IR-only NPs, respectively (M–R). Black asterisk in M shows thick, $VGLUT_2$-IR fiber bundles, from which smaller bundles appear to detach (double arrowheads in M). Black arrowheads show

TH-IR fibers. Perineuronal $VGLUT_2$-IR baskets (arrowheads in P) are occasionally seen around TH-IR NPs (arrows in Q). Scale bars: 50 μm (C=A, B); 20 μm (I= D–H; L=J, K; O=M, N; R=P, Q).

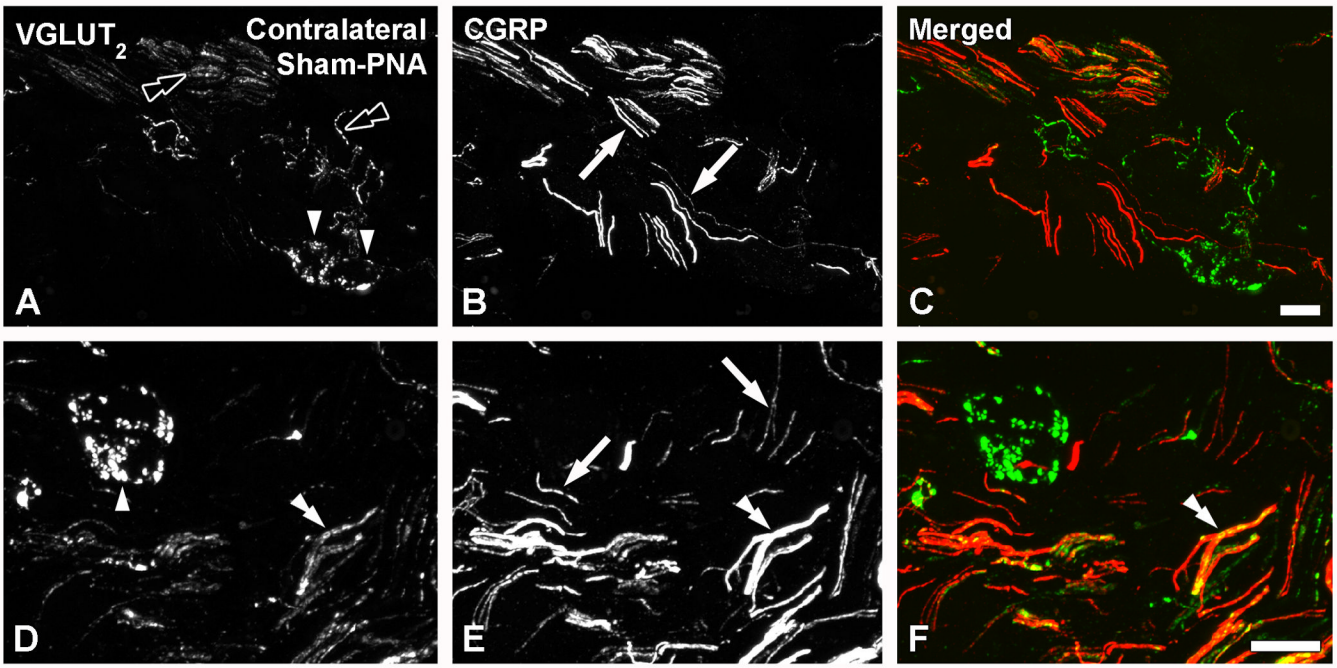

Figure 8.

Confocal immunofluorescence photomicrographs of sections of the contralateral MPGs of sham-PNA mice, co-incubated with $VGLUT_2$ (A, D) and CGRP (B, E) antisera (C, F, show merged images). Black double arrowheads in (A) and arrowheads in (A, D) show $VGLUT_2$-IR nerves or perineuronal baskets, respectively. Arrows in (B, E) and double arrowhead in (D–F) show CGRP fibers or $VGLUT_2$/CGRP-double stained nerve bundles. Scale bars: 20 μm (C=A, B; F=D, E).

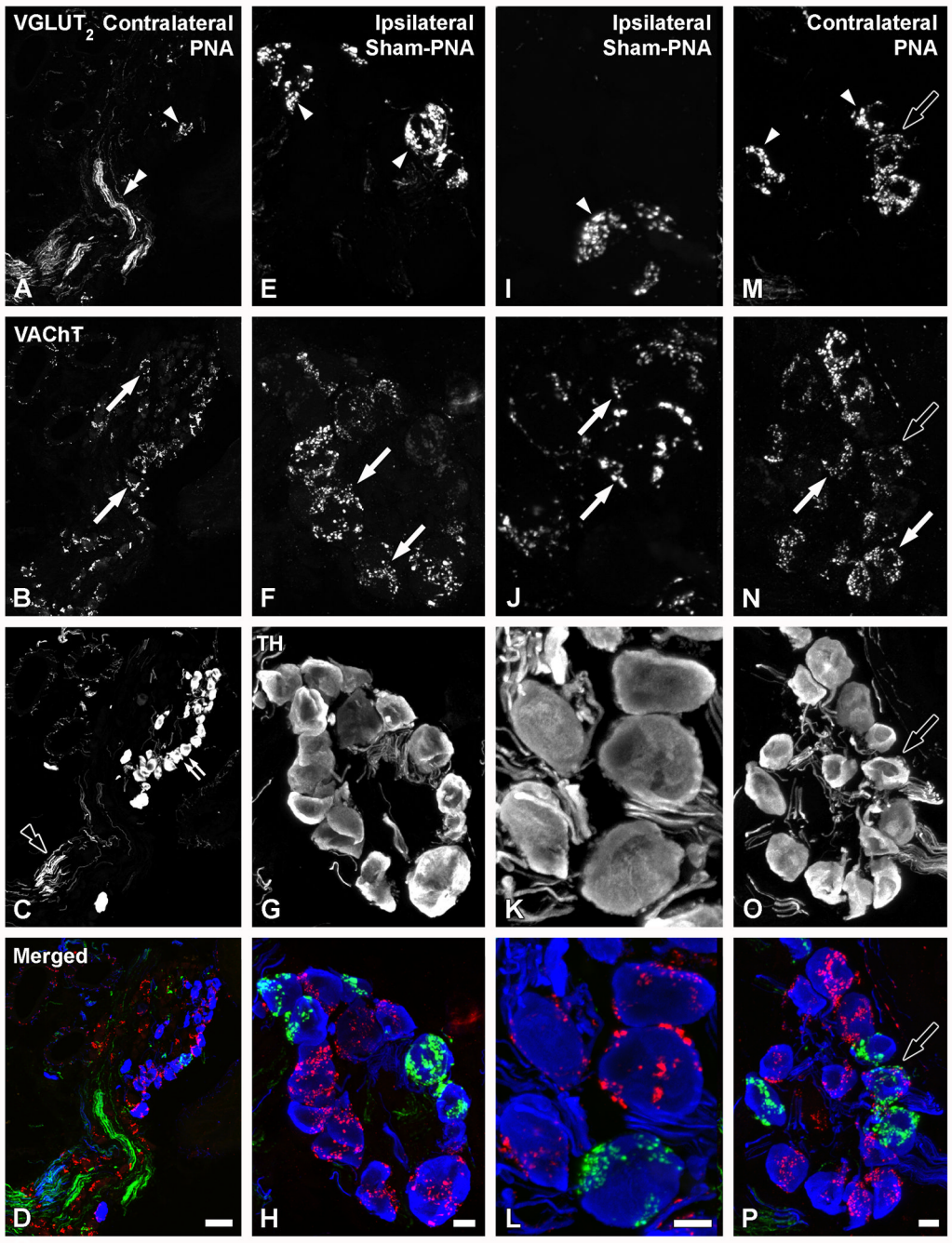

Figure 9.

Confocal immunofluorescence photomicrographs of sections from contralateral (A–D; M–P) or ipsilateral (E–L) MPGs after PNA (A–D; M–P) or sham-PNA (E–L), incubated with $VGLUT_2$ (A, E, I, M), VAChT (B, F, J, N) and TH (C, G, K, O) antisera (D, H, L, P, show merged images). Arrowheads in (A, E, I) and white arrows in (B, F, J) show two separate populations of TH-IR neurons showing $VGLUT_2$- or VAChT-IR perineuronal baskets, respectively. Double arrowhead in (A) and black double arrowhead in (C) show thick $VGLUT_2$- or TH-IR nerve bundles, respectively. Black arrows in (M–P) show some TH-IR NPs innervated by both $VGLUT_2$- and VAChT-IR baskets. Scale bars: 50 μm (D=A–C); 10 μm (H=E–G; L=I–K; P=M–O).

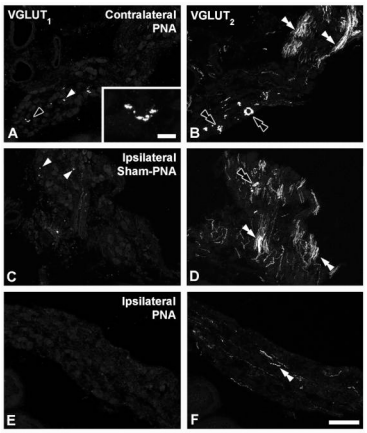

Figure 10.

Confocal immunofluorescence photomicrographs of sections from contralateral (A, B) or ipsilateral (C–F) MPGs after PNA (A, B, E, F) or sham-PNA (c, D), incubated with $VGLUT_1$ (A, C, E) or $VGLUT_2$ (B, D, F) antisera. White arrowheads in (A, C) show $VGLUT_1$-IR varicosities (shown at higher magnification in inset (black arrowhead)). White or black double arrowheads show nerve fibers (B, D, F) or perineuronal baskets (B, D), respectively. Scale bars: 100 μm (A–F); 10 μm (inset in A).

Table 1

Primary and secondary antibodies/fluorophores used for the identification of $VGLUT_1$, $VGLUT_2$, ATF-3, TH, VAChT and CGRP. Single staining was achieved using the TSA Plus technique (T). In some cases, more than one primary antibody was used for colocalization experiments (C) and thus processed with different combinations of TSA Plus and indirect immunofluorescence (I) techniques.

PRIMARY ANTIBODIES		
Target antigen and host species	**Dilution**	**Reference or source**
Rabbit anti-$VGLUT_1$	1:4,000 (T)	Kawamura et al., 2006
Guinea Pig anti-$VGLUT_2$	1:8,000 (T)	Miyazaki et al., 2003; Brumovsky et al., 2007
Rabbit anti-ATF-3	1:8,000 (T)/ 1:400(C; I)	sc-188; Santa Cruz
Rabbit anti-TH	1:4,000 (T) / 1:400 (C; I)	AB152; Millipore
Goat anti-VAChT	1:4,000(C; T)	AB1578; Millipore
Rabbit anti-CGRP	1:60,000 (C; T)	C8198; Sigma
SECONDARY ANTIBODIES / FLUOROPHORES		
HRP-donkey anti-rabbit	1:200	711-035-152; Jackson Immunoresearch
HRP-donkey anti-guinea pig	1:200	706-035-148; Jackson Immunoresearch
HRP-donkey anti-goat	1:200	805-035-180; Jackson Immunoresearch
TRITC-donkey anti-rabbit	1:400	711-025-152; Jackson Immunoresearch
Cyanine 5-donkey anti-rabbit	1:600	711-175-152; Jackson Immunoresearch
Fluorescein tyramide	1:200	NEL741; Perkin Elmer
Tetramethylrhodamine tyramide	1:600	NEL742; Perkin Elmer

Table 2

Percentage of LSC NPs expressing $VGLUT_1$, $VGLUT_2$ or $VGLUT_3$ mRNAs in naïve, sham-PNA, contralateral PNA (Cont-PNA), ipsilateral-PNA (Ipsi-PNA); sham SNA, Cont-SNA or Ipsi-SNA.

	Naïve (n=4)	Sham-PNA (n=2)	Cont-PNA (n=3)	Ipsi-PNA (n=4)	Sham-SNA (n=2)	Cont-SNA (n=1)	Ipsi-SNA (n=4)
$VGLUT_1$	0	0	0	0	0	0	0
$VGLUT_2$	0	0.2 ± 0.1 %	0.4 ± 0.4 %	7 ± 1.6 %**;†	0	0	3 ± 1 %*
$VGLUT_3$	0	0	0	0	0	0	0

*† $P<0.05$;

** $P<0.01$.

* compares naïve vs. Ipsi-SNA;

** compares naive vs. Ipsi-PNA;

† compares Cont- vs. Ipsi PNA.